Surface entropy in statistical emission of massive fragments from equilibrated nuclear systems

Jan Tõke, Jun Lu, and W. Udo Schröder
Department of Chemistry, University of Rochester, Rochester, New York 14627
(Received 23 July 2002; published 24 March 2003)

Statistical fragment emission from excited nuclear systems is studied within the framework of a schematic Fermi-gas model combined with Weisskopf's detailed balance approach. The model considers thermal expansion of finite nuclear systems and pays special attention to the role of the diffuse surface region in the decay of hot equilibrated systems. It is found that with increasing excitation energy, effects of surface entropy lead to a systematic and significant reduction of effective emission barriers for fragments and, eventually, to the vanishing of these barriers. The model predicts a maximum (effective) nuclear temperature and the occurrence of negative nuclear heat capacities, effects that have been reported in the literature. It also accounts for the observed linearity of pseudo-Arrhenius plots of the logarithm of the fragment emission probability *versus* the inverse square root of the excitation energy, but does not predict true Arrhenius behavior of these emission probabilities.

DOI: 10.1103/PhysRevC.67.034609 PACS number(s): 21.65.+f, 21.60.Ev, 25.70.Pq

I. INTRODUCTION

Over the last decade, considerable efforts have been made to understand the phenomenon of the production of multiple intermediate-mass fragments (IMF) in individual nuclear reaction events. As a contribution to these continuing efforts, the present study demonstrates that a simple scenario, closely related to that known from fission studies, offers an explanation of how, at moderately high excitation energies, IMF emission can compete effectively with nucleon evaporation. It represents an extension of ideas and formalism presented in a recent publication [1]. Central to this formalism is the notion of a relatively high entropy associated with the diffuse nuclear surface region (as opposed to bulk matter).

The model formalism adopted in the present study is described in detail in Section II. While this formalism is somewhat schematic, it is believed to capture the essential physics underlying the processes involved. One benefit of such a schematic treatment is that it provides direct insight into the phenomena of interest, disregarding a multitude of secondary details demanded by a more rigorous approach. Results of calculations are presented in Sec. III, while the conclusions are presented in Sec. IV.

II. THEORETICAL FORMALISM

The present study assumes that an excited nuclear system expands in a self-similar fashion so as to reach a state of approximate thermodynamic equilibrium, where the entropy S is maximal for the given total excitation energy E^*_{tot}, i.e.,

$$\left.\frac{\partial S(E^*_{tot},\rho)}{\partial \rho}\right|_{E^*_{tot}} = 0. \tag{1}$$

The functional dependence of the entropy on E^*_{tot} and bulk nuclear matter density ρ is evaluated using the Fermi-gas model relationship

$$S = 2\sqrt{aE^*_{th}} = 2\sqrt{a(E^*_{tot} - E_{compr})}, \tag{2}$$

where a is the level density parameter, E^*_{th} is the thermal excitation energy, and E_{compr} is the collective compressional energy. The dependence of S on bulk nuclear matter density ρ arises in Eq. (2) through the dependence of both, the level density parameter a (''little-a'') and the compressional energy E_{compr} on the matter density.

The dependence of little a on the nuclear matter density for infinite nuclear matter is given by the Fermi-gas model:

$$a = a_o\left(\frac{\rho}{\rho_o}\right)^{-2/3}, \tag{3}$$

where a_o is the level density parameter for the nuclear matter at ground-state matter density ρ_o.

The above equation holds approximately also for finite nuclei if the expansion or compression of these nuclei is assumed to occur in a self-similar fashion. This is so because for finite nuclei, the little-a parameter consists [2,3] of volume and surface terms, a_V and a_σ, respectively, both of which are proportional to $\rho^{-2/3}$ under the assumption of self-similar expansion:

$$a = a_V + a_\sigma = A\left(\frac{\rho}{\rho_o}\right)^{-2/3}\alpha_V + A^{\frac{2}{3}}\left(\frac{\rho}{\rho_o}\right)^{-2/3}\alpha_\sigma, \tag{4}$$

where α_V and α_σ are volume and surface coefficients, respectively, independent of bulk nuclear matter density.

The term ''self-similar expansion'' is used here to describe a type of expansion in which any change in the matter density profile is reducible to a simple rescaling of the radial coordinate, such that

$$f_\rho(r) = c^3 f_o(cr), \tag{5}$$

where $f_o(r)$ is the ground-state density profile function and c is a scaling constant.

The presence of a surface contribution to the level density parameter is of crucial importance in the present study as it describes that part S_σ of the entropy S of the system, which

is associated with the diffuse surface domain and is seen to have significant effect on the fragment emission probability. One has

$$S = S_V + S_\sigma , \tag{6}$$

where S_V is the entropy of the bulk matter.

The compressional energy in Eq. (2) is approximated in the present study following the schematic prescription proposed in the expanding emitting source model EESM [4], i.e.,

$$\epsilon_{compr} = \epsilon_b \left(1 - \frac{\rho}{\rho_o} \right)^2 , \tag{7}$$

where ϵ_{compr} and ϵ_b are the compressional and the ground-state binding energies per nucleon of the system, respectively. Note that Eq. (7) ensures that the compressional energy varies parabolically with ρ, from zero at ground-state density ρ_o to ϵ_b at zero density.

Equations (1)–(3) and (7) allow one to obtain an analytical expression for the equilibrium density ρ_{eq}/ρ_o of nuclear matter as a function of the excitation energy per nucleon, $\epsilon^*_{tot} = E^*_{tot}/A$, where A is the mass number of the system:

$$\frac{\rho_{eq}}{\rho_o} = \frac{1}{4} \left(1 + \sqrt{9 - 8 \frac{\epsilon^*_{tot}}{\epsilon_b}} \right) . \tag{8}$$

Equation (8) reflects the fact that for $\epsilon^*_{tot} < \epsilon_b$, the system is bound, as far as the self-similar expansion mode is concerned, and features a single maximum entropy for the range of matter densities $1/2 \leqslant \rho_{eq}/\rho_o \leqslant 1$. For $\epsilon^*_{tot} \geqslant \epsilon_b$, the system is essentially unbound with respect to the self-similar expansion mode, with the entropy diverging, as the matter density ρ tends to zero. However, for $(9/8)\epsilon_b \geqslant \epsilon^*_{tot} \geqslant \epsilon_b$, the system still has a local, metastable maximum at a finite density given by Eq. (8), i.e., in the range of matter densities $1/4 \leqslant \rho_{eq}/\rho_o \leqslant 1/2$. The latter metastable (with respect to self-similar expansion mode) maximum in entropy is separated from the divergence at zero density by a minimum at ρ_{saddle}, where

$$\frac{\rho_{saddle}}{\rho_o} = \frac{1}{4} \left(1 - \sqrt{9 - 8 \frac{\epsilon^*_{tot}}{\epsilon_b}} \right) . \tag{9}$$

Here, $E_b = A\epsilon_b$.

The probability p of emitting a fragment from an equilibrated excited system, as defined above, can be evaluated using the Weisskopf formalism [5]:

$$p \propto e^{\Delta S} = e^{S_{saddle} - S_{eq}}, \tag{10}$$

where S_{saddle} and S_{eq} are saddle-point and equilibrium-state entropies, respectively. The latter two entropies can be calculated using Eq. (2),

$$S_{eq} = 2 \sqrt{a_A \left[E^*_{tot} - E_b \left(1 - \frac{\rho_{eq}}{\rho_o} \right)^2 \right]} , \tag{11}$$

$$S_{saddle} = S_{res} + S_{frag} = 2 \sqrt{(a_{res} + a_{frag}) E^{*th}_{saddle}} . \tag{12}$$

In Eqs. (11) and (12), a_A, a_{res} and a_{frag} are the level density parameters of the system at equilibrium, the residue, and the fragment, respectively, while E^{*th}_{saddle} is the thermal excitation energy of the system in the saddle-point configuration. The latter quantity is calculated as

$$E^{*th}_{saddle} = E^*_{tot} - E_b \left(1 - \frac{\rho_{eq}}{\rho_o} \right)^2 - V_{saddle} , \tag{13}$$

where V_{saddle} is the (collective) saddle-point energy.

Note that the present formalism of statistical decay of excited nuclear systems, albeit schematic, makes no use of intensive parameters, such as temperature or pressure. As evident from Eqs. (1)–(13), the present model builds entirely on extensive variables, both thermostatic (total excitation energy, compressional energy, and entropy) and geometrical (density parameter ρ, used here to describe the volume of the system). This is in a stark contrast to many approaches commonly used to describe statistical decay of nonextensive systems, i.e., systems for which the thermodynamic limit cannot be reached. These latter approaches include the equilibrium statistical model Gemini [6], the expanding emitting source model [4], Fisher's model [7], and the Arrhenius-type Berkeley approach [8], all of which rely inherently on the notion of a temperature, an intensive parameter. While the above statements should not be construed as a criticism of the cited models, it had been argued [9] that, thermodynamical models based on extensive observables, such as entropy, total excitation energy, and geometry, are better suited for the purpose of nonextensive thermostatics of ''small'' systems than models built on intensive parameters.

While not constituting an inherent element of the present model, the notion of a (microcanonical or effective) nuclear temperature is used in the following section to discuss a caloric curve—an entity that has attracted much attention in the course of multifragmentation studies [10,11]. The notion of an (effective) temperature has been used also in constructing an Arrhenius plot for fragment emission probabilities, another entity that has attracted much attention in recent years [8]. While using the notion of an effective temperature, however, one has to keep in mind its possible limitations as far as the description of nonextensive systems is concerned. For the above specific application, an effective nuclear temperature can be obtained from the commonly used Fermi-gas model relationship between the temperature T and thermal excitation energy E^*_{th}:

$$T = \sqrt{\frac{E^*_{th}}{a}} = \left(\frac{\rho_{eq}}{\rho_o} \right)^{1/3} a_o^{-1/2} \sqrt{E^*_{tot} - E_b \left(1 - \frac{\rho_{eq}}{\rho_o} \right)^2} . \tag{14}$$

To allow one to quickly evaluate the magnitude of the effects due to surface entropy, the notion of an effective barrier B_{eff} determining the emission probability p is used in

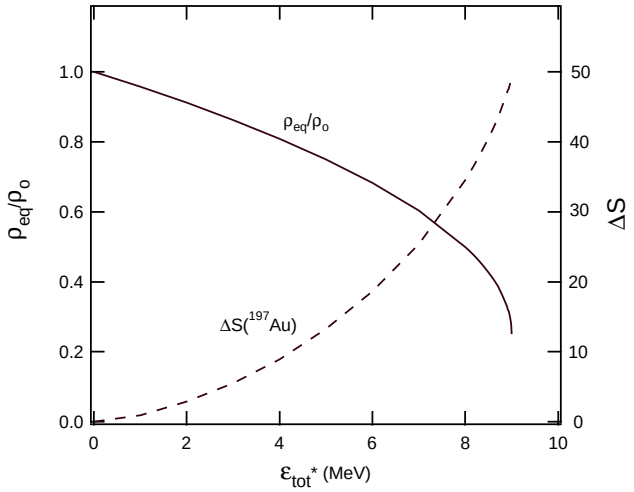

FIG. 1. Equilibrium density of bulk nuclear matter (solid curve) and the net gain in entropy realized by an ^{197}Au system as a result of the relaxation of the self-similar expansion mode (dashed curve), plotted as functions of total excitation energy per nucleon.

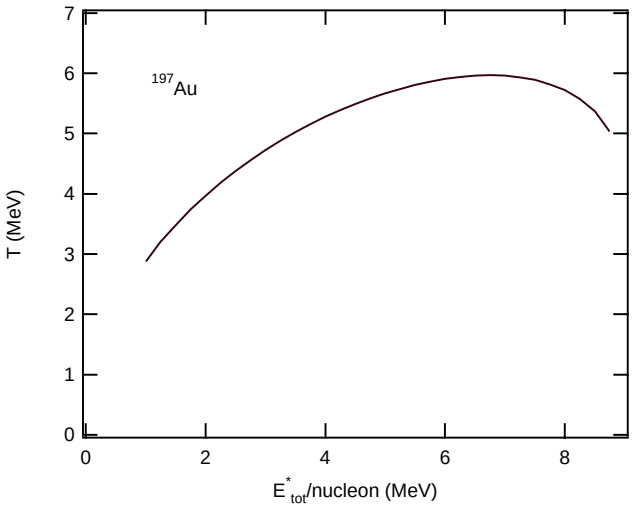

FIG. 2. Caloric curve for the ^{197}Au system.

the following section. This notion is introduced so as to formally reduce the emission probability p given by Eqs. (10)–(12) of the present formalism to a more intuitive, effective Boltzmann factor. The effective barrier is defined by the equation

$$p \propto e^{-B_{eff}/T}, \tag{15}$$

and hence,

$$B_{eff} = -T\Delta S. \tag{16}$$

Note again that Eq. (16) does not include any intensive parameters, the parameter T being constructed from purely extensive observables [see Eq. (14)].

A selection of results of calculations performed using the above formalism is presented in Sec. III below.

III. RESULTS OF MODEL CALCULATIONS

Results of the calculations performed in the framework of the formalism presented in Sec. II are presented in Figs. 1–7. In these calculations, values of $\alpha_V = 1/14.6$ MeV^{-1} and $\alpha_\sigma = 4/14.6$ MeV^{-1} have been assumed for the coefficients α_V and α_σ, as suggested in the literature [2]. Further, $\epsilon_b = 8$ MeV was assumed [4] for the ground-state binding energy per nucleon, while the saddle-point collective energy was approximated by the Coulomb energy of the residue and fragment represented by two touching spheres of radius parameter $r_{Coul} = 1.3(\rho/\rho_o)^{-1/3}$ fm. The calculations were made for excited ^{197}Au nuclei.

Figure 1 illustrates the dependence of the equilibrium density ρ_{eq} of bulk matter on the excitation energy per nucleon (solid curve). As seen in this figure, for the range of excitation energies readily accessible in experiments, the bulk matter density in a state of maximum entropy differs substantially from that of the nuclear ground state. This affects both, the caloric equation of state and the fragment emission probability, two entities of considerable interest.

The dashed curve seen in Fig. 1 illustrates the net gain in entropy resulting from the relaxation of the self-similar expansion mode in an excited ^{197}Au system. Large gains in entropy associated with the relaxation of this mode emphasize the importance of this mode for a statistical description of excited nuclear systems, notably for models based on the concept of microcanonical [12] or pseudomicrocanonical [13] equilibrium.

The caloric curve calculated for states of maximum entropy, i.e., for the states of equilibrium density ρ_{eq}, is depicted in Fig. 2. Not surprisingly, this curve shows considerable deviation from the simple Fermi-gas form of $T \propto \sqrt{E^*_{tot}}$. Note that in experiments such as the recently reported ISIS experiment [14], it is E^*_{tot} and not the purely

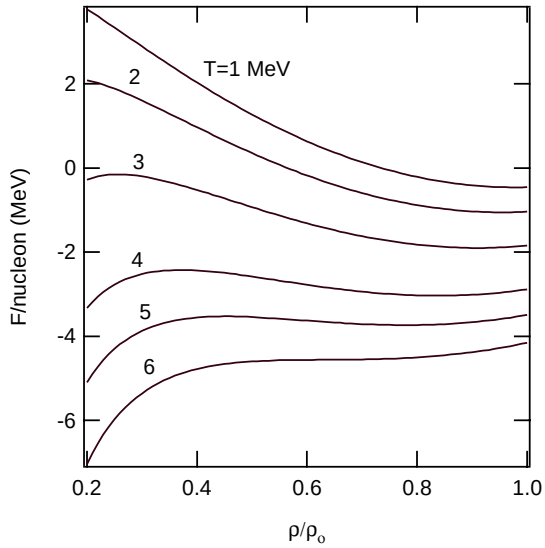

FIG. 3. Free energy for the ^{197}Au system as a function of nuclear matter density and temperature.

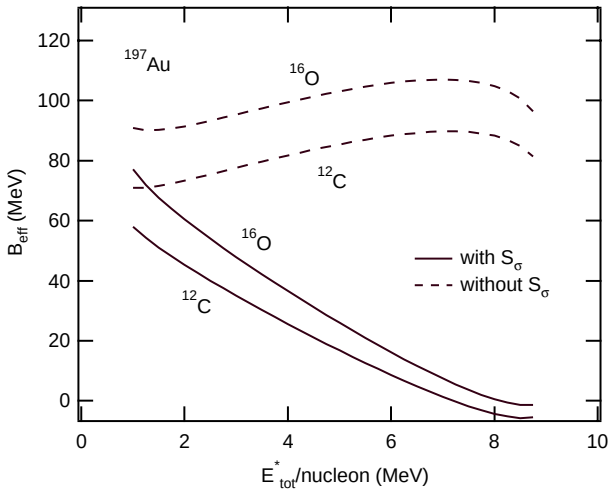

FIG. 4. Effective barriers for the emission of ^{12}C and ^{16}O fragments from equilibrated excited ^{197}Au systems as functions of excitation energy per nucleon.

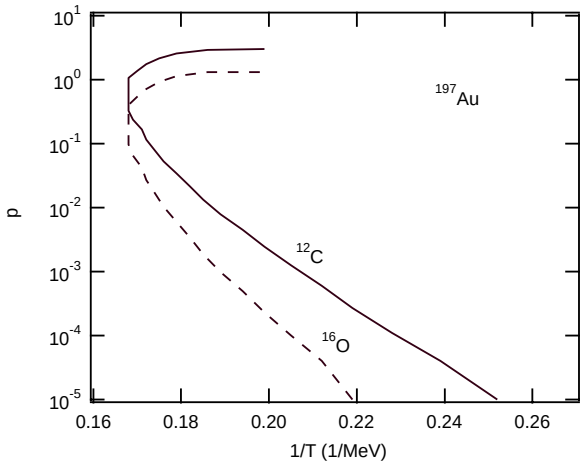

FIG. 6. Arrhenius plots for emission of ^{12}C and ^{16}O fragments from excited ^{197}Au systems.

thermal contribution to it, E^*_{th}, that is in fact measured. This is so, because the static compressional energy E_{compr} is experimentally undistinguishable from thermal excitation E^*_{th}.

Most notably, the caloric curve predicted in Fig. 2 features a maximum temperature of approximately $T_{max}=6$ MeV. This is an indication that, for higher temperatures, the system is inherently unstable and does not find an equilibrium density. In other words, under the assumption that its matter distribution is homogeneous, a nuclear system placed in a heat bath of $T>6$ MeV would expand indefinitely, for which it would derive increasing amounts of energy from the heat bath. In a more realistic case, which is beyond the present consideration, before reaching thermal equilibrium, the system would likely decay dynamically into a ''gas'' of fragments and free nucleons that would continue its indefinite expansion. It is worth noting that, in the present formalism, a limiting, maximum nuclear temperature arises naturally from the requirement of the dynamical equilibrium implied by Eq. (1). This is in contrast to many other statistical-decay models for excited nuclear systems, notably to all models relying on the concept of the existence of a freezeout volume [12,13] or a breakup configuration [15]. It is also in contrast to Fisher's model [7], which has recently been reconsidered in the context of intermediate-mass fragment production [16]. None of the above model approaches [7,12,13,15,16] predicts a maximum temperature. However, the existence of such a limiting temperature appears to be supported by a series of experimental observations [10].

The particular form of the caloric curve seen in Fig. 2 can, perhaps, be better understood when inspecting the dependence of the free energy F on matter density ρ and temperature T, which is is illustrated in Fig. 3. The calculations show

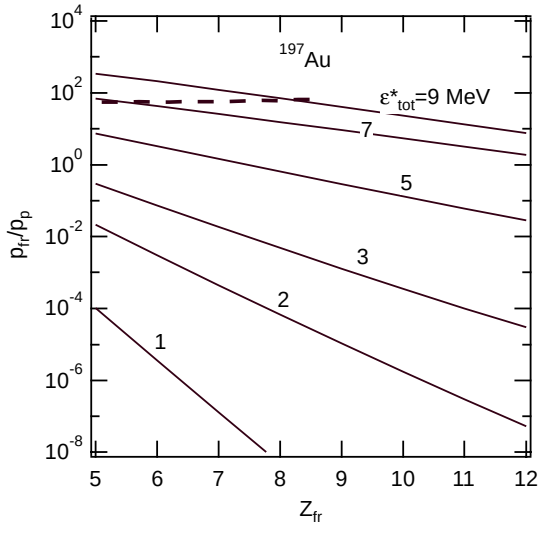

FIG. 5. Distributions of relative emission probabilities of various IMFs from an excited, equilibrated ^{197}Au system as functions of the total excitation energy (solid curves). The dashed line represents the boundary of the domain of dynamical instability of the system (see text).

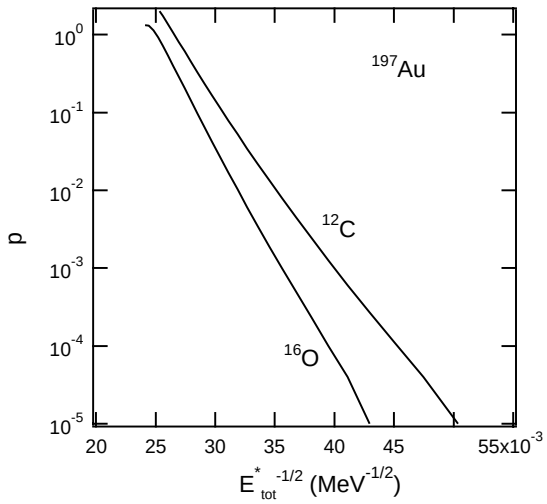

FIG. 7. Pseudo-Arrhenius plots for emission of ^{12}C and ^{16}O fragments from excited ^{197}Au systems.

that, at temperatures below $T \approx 6$ MeV, the free energy as a function of ρ features two equilibrium points, a local minimum and a local maximum, where the latter reflects an unstable equilibrium These two points, predicted for any temperature T of less than approximately 6 MeV, correspond to different excitation energies per nucleon, ϵ^*_{tot}. Note that at both these extremal points, the pressure of the system at its surface is zero. This is so, because the pressure is proportional to the partial derivative of the free energy with respect to density at constant entropy, and since both, the free energy and the entropy, are stationary with respect to the matter density at the extremal points in question. At $T \approx 6$ MeV, the minimum and the maximum in $F(\rho)$ merge into an inflection point. At even higher temperatures, the free energy features only a monotonic decrease with decreasing ρ. The inflection point in F for ($T \approx 6$ MeV) corresponds to a maximum of T as a function of E^*_{tot}. Obviously, a monotonic decrease in free energy with decreasing matter density for a given temperature implies that no equilibrium density exists for that temperature.

The role of the surface entropy in fragment emission is clear from Fig. 4 illustrating the dependence of effective barriers [see Eq. (16)] for the emission of ^{12}C and ^{16}O from exited ^{197}Au nuclei. Solid lines in this figure illustrate the results obtained when the surface entropy is taken into consideration via inclusion of a_σ in the expression for the level density parameter a [see Eq. (3)], while dashed lines represent results of calculations in which the surface entropy effects were neglected, i.e., in which a was assumed simply proportional to the mass number.

It is important to note that, with the reduction in the effective barrier being dominantly due to surface entropy effects, no analogous reduction is expected for the emission of nucleons or light charged particles. In the latter case, the effective barriers are expected to show trends similar to those shown by the dashed lines in Fig. 4.

The effects of the surface entropy on the relative emission rates of various IMFs are illustrated in Fig. 5, displaying the reduced probabilities (taken as bare Boltzmann factors) for the emission of IMFs of different atomic numbers from an equilibrated ^{197}Au system as functions of the total excitation energy per nucleon. In the calculations, it was assumed that the mass numbers of the fragments equal twice their atomic numbers, i.e., $A_{fr} = 2Z_{fr}$. The spectra are normalized to the probability for emitting a proton, bound to the system by $Q_p = 8$ MeV and experiencing a Coulomb barrier of 4 MeV (corresponding to a Coulomb radius parameter of $r_C = 1.3$ fm). As seen in this figure, already at excitation energies per nucleon of the order of 3 MeV/nucleon, fragment emission begins to compete effectively with proton emission and, then, at higher excitation energies, fragment emission becomes the dominant decay mode. Note, that the highest probabilities seen in Fig. 5, i.e., those depicted above the dashed line, reflect a dynamical system instability with respect to the fragment emission mode. In fact, Weisskopf's approach [5] is inapplicable in the domain above the dashed line, as in this domain, the saddle-point entropy exceeds that for the "equilibrium" density of a self-similarly expanded system.

Since the magnitude of the effective barrier for IMF emission depends on the excitation energy and, thus, on temperature T, and since T is a nonmonotonic function of E^*_{tot}, one would expect the fragment emission probabilities p to deviate significantly from a simple Arrhenius law with an exponential functional dependence on the inverse temperature $1/T$. This expectation is confirmed by Fig. 6, where logarithmic plots of p versus $1/T$ are seen to feature clear deviations from linearity, including a prominent "back-bending." The latter backbending is obviously expected, in view of the maximum in the caloric curve seen in Fig. 2. Such a behavior is also suggested by the general deviation of the caloric equation of state from the one for a low-temperature Fermi gas.

On the other hand, pseudo-Arrhenius plots depicted in Fig. 7, where the logarithm of the emission probability, $\ln(p)$, is plotted versus the inverse square root of the total excitation energy, $1/\sqrt{E^*_{tot}}$, are to a good approximation straight lines. This observation comes as a surprise, as it cannot readily be expected, based on the details of the theoretical formalism employed. Therefore, no simple explanation for such a linearity can be offered at this time, the very rationale behind the construction of such pseudo-Arrhenius plots being numerous experimental findings [8,17–20]. While it may be purely fortuitous, the linear character of pseudo-Arrhenius plots predicted by the present model seems to be in agreement with experimental observations.

IV. CONCLUSIONS

A model has been developed to describe quantitatively, albeit in a schematic fashion, a scenario of purely statistical emission of massive fragments from finite equilibrated systems. The formalism is based on the use of extensive observables only, complemented by the geometry of the used phase space. It is, hence, free of the possible limitations of models relying on intensive variables. The presented formalism recognizes the importance of thermal expansion of hot matter and considers the stability of such systems at equilibrium nuclear densities. Unlike many other models and approaches, the present formalism predicts in a natural fashion a limiting maximum temperature bound nuclear system can sustain, an effect supported by numerous experimental observations. The important role of surface entropy consists in an effective "softening" of the nuclear surface, resulting in enhanced fragment emission probabilities. The decay scenario underlying this formalism is that of a thermally expanded system with developed thermal fluctuations of the diffuse surface.

Note added in proof. It came to our attention that the curve ρ_{eq}/ρ_0 (cf. Fig. 1) obtained from the single-parameter function in Eq. (8) essentially coincides with a similar curve resulting from a finite-temperature Hartree-Fock calculation, as reported in Ref. [21].

ACKNOWLEDGMENTS

This work was supported by the U.S. Department of Energy Grant No. DE-FG02-88ER40414.

[1] J. Tõke and W.U. Schröder, Phys. Rev. Lett. **82**, 5008 (1999).
[2] J. Tõke and W.J. Swiatecki, Nucl. Phys. **A372**, 141 (1981).
[3] A.V. Ignatyuk *et al.*, Sov. J. Nucl. Phys. **21**, 612 (1975).
[4] W.A. Friedman, Phys. Rev. Lett. **60**, 2125 (1988).
[5] V.F. Weisskopf, Phys. Rev. **52**, 295 (1937).
[6] R.J. Charity, computer code GEMINI, see wunmr.wustl.edu/pub/gemini
[7] M.E. Fisher, Physics (N.Y.) **3**, 255 (1967).
[8] L.G. Moretto *et al.*, Phys. Rep. **287**, 249 (1997).
[9] D.H.E. Gross, Nucl. Phys. **A681**, 366 (2001).
[10] J.B. Natowitz *et al.*, Phys. Rev. C **65**, 034618 (2002).
[11] J.B. Natowitz *et al.*, Phys. Rev. Lett. **89**, 212701 (2002).
[12] D.H.E. Gross, Phys. Rep. **279**, 119 (1997).
[13] J.P. Bondorf *et al.*, Phys. Rep. **257**, 133 (1995).
[14] L. Beaulieu *et al.*, Phys. Rev. C **63**, 031302(R) (2001).
[15] S. Albergo, S. Costa, E. Costanzo, and A. Rubbino, Nuovo Cimento Soc. Ital. Fis., A **89**, 1 (1985).
[16] J.B. Elliott *et al.*, Phys. Rev. Lett. **88**, 042701 (2002).
[17] L.G. Moretto *et al.*, Phys. Rev. Lett. **74**, 1530 (1995).
[18] K. Tso *et al.*, Phys. Lett. A **361**, 25 (1997).
[19] L. Beaulieu, L. Phair, L.G. Moretto, and G.J. Wozniak, Phys. Rev. Lett. **81**, 770 (1998).
[20] L.G. Moretto, L. Phair, and G.J. Wozniak, Phys. Rev. C **60**, R031601 (1999).
[21] J. B. Natowitz *et al.*, Phys. Rev. C **66**, 031601(R) (2002).